Received: 22 December 2022 | Revised: 16 March 2023 | Accepted: 19 March 2023

DOI: 10.1111/pce.14587

ORIGINAL ARTICLE

Plant, Cell & Environment WILEY

Deep-water uptake under drought improved due to locally increased root conductivity in maize, but not in faba bean

Yannik Müllers[1] | **Johannes A. Postma**[1] | **Hendrik Poorter**[1,2] | **Dagmar van Dusschoten**[1]

[1]IBG-2, Plant Sciences, Forschungszentrum Jülich, Jülich, Germany

[2]Department of Natural Sciences, Macquarie University, Sydney, Australia

Correspondence
Dagmar van Dusschoten, IBG-2, Plant Sciences, Forschungszentrum Jülich, Jülich, Germany.
Email: d.van.dusschoten@fz-juelich.de

Funding information
Helmholtz Association, Germany, Grant/Award Number: POF4-899; Deutsche Forschungsgemeinschaft (DFG, German Research Foundation), Grant/Award Number: 491111487

Abstract

Moderate soil drying can cause a strong decrease in the soil-root system conductance. The resulting impact on root water uptake depends on the spatial distribution of the altered conductance relatively to remaining soil water resources, which is largely unknown. Here, we analyzed the vertical distribution of conductance across root systems using a novel, noninvasive sensor technology on pot-grown faba bean and maize plants. Withholding water for 4 days strongly enhanced the vertical gradient in soil water potential. Therefore, roots in upper and deeper soil layers were affected differently: In drier, upper layers, root conductance decreased by 66%–72%, causing an amplification of the drop in leaf water potential. In wetter, deeper layers, root conductance increased in maize but not in faba bean. The consequently facilitated deep-water uptake in maize contributed up to 21% of total water uptake at the end of the measurement. Analysis of root length distributions with MRI indicated that the locally increased conductance was mainly caused by an increased intrinsic conductivity and not by additional root growth. Our findings show that plants can partly compensate for a reduced root conductance in upper, drier soil layers by locally increasing root conductivity in wetter layers, thereby improving deep-water uptake.

KEYWORDS

MRI, plant water stress, root conductance, root hydraulic architecture, root water uptake, soil drying, soil water profiler, water uptake compensation

1 | INTRODUCTION

Terrestrial plants exposed to drying soils suffer from a reduced water potential which can lead to cell turgor loss (Bartlett et al., 2012), hydraulic failure of xylem vessels (Urli et al., 2013) and impaired phloem transport (Thompson, 2006). To mitigate this, plants close stomata at the cost of reduced CO_2 gain, up to carbon starvation (McDowell, 2011). In the first place, the reduced plant water potential is caused by the drop in soil water potential. However, the plant water potential additionally depends on how the hydraulic conductance of the root system is affected by soil drying (Bourbia et al., 2021; Nobel & Cui, 1992; Rodriguez-Dominguez & Brodribb, 2020; Saliendra & Meinzer, 1989). In a recent study, we showed that even moderate soil drying can induce an exponential decline of the total root system conductance (Müllers, Postma, Poorter, & van Dusschoten, 2022). Considering the distribution along the root system of such a net decline is crucial to understand its impact on the plant water balance.

Soil drying is a highly nonuniform process and usually results in a pronounced vertical gradient with relatively dry shallow soil layers and relatively wet deep soil layers (Hillel et al., 1976; Kondo et al., 2000; Markesteijn et al., 2010). Under such conditions, water in deeper layers is much easier to extract, that is, a deep root requires a less negative xylem water potential to realize a certain water uptake rate compared with an otherwise identical shallow root. Following this rationale, effectively using deep water resources is a key to withstand droughts (Wasson et al., 2012). However, several studies emphasize that plants often fail to do so and experience severe drought stress despite a relatively high water availability in deeper root zones (Gessler et al., 2022; Passioura, 1983; Prechsl et al., 2015; Rasmussen et al., 2020). A major reason is that the root conductance (K_{root}, see Table 1 for abbreviations) in deeper layers usually is low since roots are less abundant (Haberle & Svoboda, 2015; Kemper et al., 2020; Righes, 1980) and less conductive compared with shallow roots (Dara et al., 2015; Müllers, Postma, Poorter, Kochs, et al., 2022; Zarebanadkouki et al., 2013). Therefore, a more effective acquisition of deep water would require to locally increase root conductance over time. This can be achieved by increasing root length via additional root growth in deeper layers, which has been often observed upon soil drying (Alsina et al., 2011; Asseng et al., 1998; Dubrovsky et al., 1998; Rodrigues et al., 1995; Sharp & Davies, 1985). Nevertheless, as root hydraulic traits vary among individual roots and entire root systems (Ahmed et al., 2016, 2018; Clément et al., 2022; Müllers, Postma, Poorter, Kochs, et al., 2022; Rewald et al., 2012; Steudle & Peterson, 1998), local root length only partly determines a plant's ability to use deep water. Additionally, plants can increase the intrinsic root conductivity (conductance per length) by, for example, increasing the amount of active aquaporins (Johnson et al., 2014; McLean et al., 2011).

While in deeper, wetter layers, increasing the root conductance is a reasonable strategy for an effective water usage, it might be the other way around in upper, drier soil layers. Unregulated water uptake from drying soil can result in a severe water depletion zone around the roots, strongly reduce the local soil conductivity, and thus restrict water flow from the bulk soil towards the roots (Carminati & Javaux, 2020). The drop of the local soil conductivity scales with the water potential of the bulk soil and the water uptake rate per unit root length. Therefore, locally decreasing root conductance, and thus water uptake rates, in drier soil layers might be beneficial to avoid an interruption of the hydraulic pathway between remaining water in the bulk soil and the root surface. Mechanisms like enhanced root suberization (Barrios-Masias et al., 2015; Cruz et al., 1992; Lo Gullo et al., 1998; North & Nobel, 1991), or reducing the amount of open aquaporins (Martre et al., 2001; Rodríguez-Gamir et al., 2019) enable plants to reduce root hydraulic conductance during droughts.

Following these considerations, we analyzed how previously measured changes in the total root system conductance (Müllers, Postma, Poorter, & van Dusschoten, 2022) are distributed over depth.

TABLE 1 Abbreviations as used in the article.

Term	Meaning	Unit
h	Soil matric potential	cm H_2O
K_{comp}	Compensatory root water uptake conductance	mL h^{-1} MPa^{-1}
k_h	Soil hydraulic conductivity	cm h^{-1}
K_{root}	Radial root conductance	mL h^{-1} MPa^{-1}
k_{root}	Radial root conductivity	mL h^{-1} MPa^{-1} m^{-1}
K_{sat}	Soil hydraulic conductivity at water saturation	cm h^{-1}
K_{SL}	Hydraulic conductance between soil and leaf	mL h^{-1} MPa^{-1}
K_{soil}	Soil hydraulic conductance	mL h^{-1} MPa^{-1}
K_{SR}	Local soil-root conductance	mL h^{-1} MPa^{-1}
$K_{SR,\ tot}$	Total conductance of the soil-root system	mL h^{-1} MPa^{-1}
L	Root length	m
r_0	Root radius	cm
r_b	Radial distance from the root centre defining the start of the bulk soil	cm
RWU	Root water uptake rate	mL h^{-1}
SWaP	Soil water profiler	
U_P	Plant-driven root water uptake distribution with depth	mL cm^{-3} h^{-1}
$\hat{U}_P$	Normalized plant-driven root water uptake distribution with depth	
U_S	Soil driven root water uptake redistribution	mL cm^{-3} h^{-1}
U_S'	Hypothetical U_S for assuming no local increases in K_{root}	mL cm^{-3} h^{-1}
U_{tot}	Total root water uptake rate	mL h^{-1}
V	Soil volume	cm^3
z_i	Depth of soil layer i	cm
α	Inverse of the air entry pressure	cm H_2O $^{-1}$
θ	Volumetric soil water content	%
$\frac{\partial\theta}{\partial t}$	Soil water depletion rate	mL cm^{-3} h^{-1}
λ_b	Dimensionless pore size index of the Brooks–Corey model	
τ	Brooks–Corey parameter with $\tau = -2-3\,\lambda_b$	
φ	Matrix flux potential	cm^2 h^{-1}
Ψ_{collar}	Water potential at the plant collar	MPa
Ψ_{leaf}	Leaf water potential	MPa
Ψ_{soil}	Water potential in the bulk soil	MPa
Ψ_{seq}	Equivalent soil water potential	MPa
Ψ_{sr}	Water potential at the soil-root interface	MPa

Although this spatial aspect is highly relevant for the plant water balance, it has been poorly investigated. The few studies measuring a spatial component of soil drying-induced alterations of root hydraulic traits used single roots, sampled at different depths (Johnson et al., 2014; Wan et al., 1994). Additional information comes from studies on partial root zone drying in which root hydraulic traits were either measured on single, sampled roots (McLean et al., 2011) or entire root systems divided into halves (Hu et al., 2011). These studies generally suggest that the conductance of roots in rather wet soil increases relatively to that of roots in rather dry soil. However, how the full vertical distributions of root hydraulic conductance change in response to soil drying is unknown, probably due to limitations in the available measurement technologies. Here, we used a recently developed, highly precise soil water sensor, called soil water profiler (SWaP; van Dusschoten et al., 2020), to noninvasively measure root water uptake profiles which reflect the distribution of root hydraulic conductance. We hypothesize that the root conductance decreases in upper soil layers while it increases in deeper layers as an early response to soil drying by means of active regulation by the plant. Such a response would reduce water stress by facilitating deep water usage and sustaining a hydraulic connection to remaining water resources in drier layers. In Figure 1, the hypothesized effect of soil drying on the spatial distribution of root conductance is summarized. The hypothesis was tested on pot-grown faba bean and maize plants during 4 days of soil drying. These two species were chosen because they differ in root system architecture, and water uptake rates per unit root length. Faba bean has a taproot system with comparably great water uptake rates per unit root length, whereas maize has a fibrous root system with comparably low water uptake rates per unit root length. Both factors potentially affect the distribution of remaining soil water under drought, and thus the resulting alterations of the local root conductance.

2 | MATERIALS AND METHODS

Data used in this study were obtained during an experiment described previously in Müllers, Postma, Poorter, and van Dusschoten (2022). Below, we shortly summarize the experimental design and explain the determination of the distribution of root conductance and root length in more detail.

2.1 | Experimental design

We germinated seeds of faba bean (*Vicia faba*, $n = 10$) and maize (*Zea mays*, $n = 10$), and transferred them into soil-filled PVC pipes (80% of a loamy sand collected in Kaldenkirchen, Germany (Pohlmeier et al., 2009), mixed with 20% coarse sand). PVC pipes had an inner diameter of 8.1 cm and were filled to a height of 45 cm resulting in 2.32 L of soil substrate at a bulk dry density of 1.47 kg L^{-1}. Plants

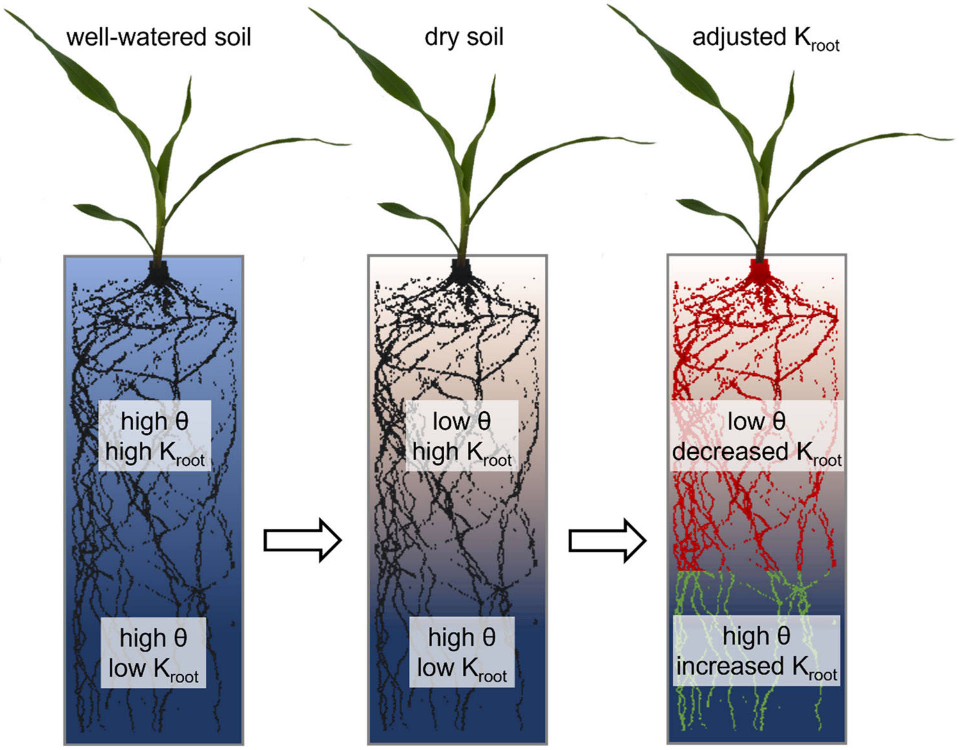

FIGURE 1 Hypothesized alterations of the spatial distribution of root hydraulic conductance (K_{root}) in response to soil drying. Usually, soil water content (θ) is reduced faster in upper than in deeper soil layers. Increasing the root conductance in deeper layers could facilitate deep water uptake while a decreasing root conductance in upper layers might prevent an interruption of water flow from the bulk soil towards the root surface.

were grown in a climate chamber at a constant temperature of 21.5 ± 0.2°C and a $\mathrm{VPD_{air}}$ of 1.49 kPa. We used a water-cooled LED panel (3200 K, 5 × 5 LEDs á 20 W) for controlled illumination of the plants. Light intensity alternated between a higher (1000 $\mu\mathrm{mol\,m^{-2}\,s^{-1}}$) and lower level (500 $\mu\mathrm{mol\,m^{-2}\,s^{-1}}$) in periods of 2 h. Each day, four high and three low light periods were applied resulting in a total of 14 h illumination and a daily light integral of 39.6 $\mathrm{mol\,m^{-2}\,day^{-1}}$. The alternating light levels were required to determine root water uptake profiles as described below. Plants were regularly watered from the top to keep the average volumetric soil water content around 20%. For fertilization, once a week an NPK nutrient salt (Hakaphos Red; Compo Expert; 8% N, 12% P, 24% K), was diluted in water at 0.3% (v/v) and used for watering. At an age between 4 and 5 weeks (thereby selecting for similar total plant water uptake rates), plants were imaged with MRI and then placed into the SWaP for continuous measurement of soil water profiles. From that moment onwards, plants were not watered anymore. Simultaneously, leaf water potential was continuously measured with a psychrometer (ICT International). After 4 days, plants were imaged with MRI again.

2.2 | Determining the normalized distribution of plant-driven root water uptake rates

For the following analysis, we interpret the 45 cm high soil columns with roots as 45 vertically stacked layers of 1 cm height. Layers are numbered with $i = 1, \ldots, 45$ from top to bottom. Upper boundary of each layer is at depth $z_i = 0, \ldots, 44$ cm. The volumetric soil water content ($\theta(z_i)$) in each layer was measured with the so-called SWaP (van Dusschoten et al., 2020). The SWaP is sensitive for the permittivity of the soil which is determined by θ. Using a calibration curve, values measured with the SWaP were converted to the local $\theta(z_i)$. Sensors of the SWaP were automatically moved along the pots with soil columns, which allowed for measuring θ-profiles in equidistant vertical steps of 1 cm every 15 min. The SWaP measurements and required data processing, is explained in more detail by van Dusschoten et al. (2020), and Müllers, Postma, Poorter, Kochs, et al. (2022).

Using this methodology, we could derive the soil water depletion rate $\left(\frac{\partial\theta(z_i,t)}{\partial t}\right)$ for each individual soil layer. $\frac{\partial\theta(z_i,t)}{\partial t}$ is determined by local root water uptake rates ($\mathrm{RWU}(z_i,t)$) and redistributive soil water flow ($\mathrm{rSWF}(z_i,t)$) between adjacent layers:

$$\frac{\partial\theta(z_i,t)}{\partial t} = \mathrm{RWU}(z_i,t) + \mathrm{rSWF}(z_i,t). \tag{1}$$

Following the hydraulic model developed by Couvreur et al. (2012), the distribution of RWU is determined by one term, solely depending on the distribution of root hydraulic conductance, and a second term additionally depending on vertical soil water gradients. We call the first term plant-driven root water uptake distributions (U_P), and the latter term soil-driven root water uptake redistribution (U_S):

$$RWU(z_i) = U_\mathrm{P}(z_i) + U_\mathrm{S}(z_i). \tag{2}$$

Under the hypothetical conditions of a uniform soil water potential over depth, U_P is equal to RWU. Across the whole pot, U_P integrates to the total root water uptake rate (U_tot). U_S is a correction term which is negative in relatively dry soil layers (local soil water potential below pot average) and positive in relatively wet soil layers (local soil water potential above pot average). Across the whole pot, U_S integrates to zero. Using these definitions and summarizing U_S and rSWF as soil water redistribution through soil and roots (S_R), Equation (1) writes:

$$\frac{\partial\theta(z_i,t)}{\partial t} = \hat{U}_\mathrm{P}(z_i)\cdot\frac{U_\mathrm{tot}(t)}{V} + S_\mathrm{R}(z_i,t). \tag{3}$$

In Equation (3) we used the normalized plant-driven root water uptake distribution ($\hat{U}_\mathrm{P}$) with $\hat{U}_\mathrm{P}(z_i) = \frac{U_{\mathrm{P}(z_i)}}{U_\mathrm{tot}}$ and the total pot volume V. Given a data set with varying U_tot, $\hat{U}_\mathrm{P}$, according to Equation (3), can be derived by a linear regression between $\frac{\partial\theta(z_i,t)}{\partial t}$ and U_tot if variations in U_tot and S_R are independent. Decoupling of variation in U_tot and S_R is achieved by the fluctuating light intensity in periods of 2 h. Assuming that changes in the soil water distribution are negligible on short time scales, a change in light intensity causes a rapid response in U_tot without affecting S_R. Thus, for data measured during a fluctuating light intensity, the slope of $\frac{\partial\theta(z_i,t)}{\partial t}$ (U_tot) is $\hat{U}_\mathrm{P}$. Since $\hat{U}_\mathrm{P}$ is determined by the distribution of root conductance, this can be understood as follows: The greater the root conductance in a specific soil layer, the greater the change in the local soil water depletion rate induced by a change in transpiration rate. The linear regression, and thus determination of $\hat{U}_\mathrm{P}$, was performed at each day separately, covering data from 12 h of alternating light. Supporting Information: Figure 1 shows the process of deriving $\hat{U}_\mathrm{P}$ profiles from the SWaP data for an exemplary maize plant at Day 1 and Day 4 of the soil drying period.

2.3 | Determining the distribution of soil water potential

The soil matric potential (h) was calculated from θ values measured with the SWaP, using a water retention curve, fitted with a Brooks–Corey model. This water retention curve has been reported in Müllers, Postma, Poorter, and van Dusschoten (2022). To obtain the distribution of soil water potential (Ψ_soil), h was corrected for gravity.

2.4 | Determining the distribution of root hydraulic conductance

To derive the spatial distribution of root hydraulic conductance (K_root), the normalized $\hat{U}_\mathrm{P}$, containing the spatial component of K_root, needs to be multiplied by the total conductance of the root system. Table 2 shows data on U_tot, leaf water potential (Ψ_leaf), the equivalent soil water potential (Ψ_seq), and the resulting total conductance between soil and leaf (K_SL) separately averaged across each day of the measurement. A detailed

TABLE 2 Total root water uptake rate (U_{tot}), leaf water potential (Ψ_{leaf}), equivalent soil water potential (Ψ_{seq}), and the resulting, total conductance between soil and leaf (K_{SL}), averaged for each day of soil drying.

	Faba bean		Maize	
Day	U_{tot} (mL h^{-1})	Ψ_{leaf} (MPa)	U_{tot} (mL h^{-1})	Ψ_{leaf} (MPa)
1	4.85 ± 0.41^a	-0.62 ± 0.05^a	4.09 ± 0.58^a	-0.55 ± 0.05^a
2	3.75 ± 0.70^a	-0.76 ± 0.04^b	3.94 ± 0.77^a	-0.64 ± 0.14^a
3	2.47 ± 0.42^b	-0.93 ± 0.07^b	3.51 ± 0.54^{ab}	-0.71 ± 0.17^a
4	1.64 ± 0.31^c	-1.11 ± 0.09^c	3.10 ± 0.43^b	-1.05 ± 0.19^b

	Faba bean		Maize	
Day	Ψ_{seq} (MPa)	K_{SL} (mL h^{-1} MPa^{-1})	Ψ_{seq} (MPa)	K_{SL} (mL h^{-1} MPa^{-1})
1	-0.02 ± 0.01^a	8.27 ± 1.12^a	-0.02 ± 0.00^a	8.73 ± 4.07^a
2	-0.04 ± 0.01^b	5.15 ± 1.30^b	-0.03 ± 0.01^b	6.55 ± 2.43^a
3	-0.08 ± 0.02^c	2.87 ± 0.56^c	-0.05 ± 0.01^c	5.67 ± 2.21^{ab}
4	-0.12 ± 0.03^d	1.57 ± 0.37^d	-0.07 ± 0.03^c	3.34 ± 1.45^b

Note: Values are species medians with median absolute deviations.

analysis of these data, especially of the exponential decline in K_{SL} in response to soil drying, is provided by Müllers, Postma, Poorter, and van Dusschoten (2022). In the present study, the data on K_{SL} were used to approximate the total conductance of the root system. For this, we assumed that the axial conductance of the shoot between root system and leaf is much greater than the total conductance of the soil-root system ($K_{SR,\,tot}$). This assumption is justified in wet soil, where radial root conductance is usually limiting water uptake (Frensch & Steudle, 1989; Reid & Hutchison, 1986; Steudle & Peterson, 1998). During soil drying, the axial shoot conductance can be reduced due to xylem embolism, and thus become an important determinant of K_{SL}. However, considerable reduction of the axial conductance due to xylem embolism in maize were measured at a soil water potential of −0.25 MPa (Ryu et al., 2016), stem water potential of −1.0 MPa (Li et al., 2009) and leaf water potential of −1.5 MPa (Cochard, 2002). Comparable values of Ψ_{leaf} were not reached in our measurements (Table 2), indicating that axial shoot conductance was not limiting for a large part of the measurement, similar to the findings of two recent studies (Corso et al., 2020; Rodríguez-Gamir et al., 2019). Therefore, we can approximate K_{SL} by $K_{SR,\,tot}$, and derive the local soil-root conductance (K_{SR}) in each layer:

$$K_{SR}(z_i) = K_{SL} \cdot \hat{U}_P(z_i). \tag{4}$$

For an overview of the hydraulic network model and the terminology used here, see Supporting Information: Figure 2. K_{SR} is composed of the local soil hydraulic conductance (K_{soil}), and the local root conductance (K_{root}), connected in series. In Supporting Information: Appendix 1, we explain two different methods to estimate the hydraulic conductance of K_{soil}. These estimations indicated that for a large part of the measurement, K_{soil} in each layer was much greater than K_{SR} (Supporting Information: Figure 3), and K_{SR} was largely determined by K_{root}. Thus, K_{root} can be reliably approximated by K_{SR}, as determined in Equation (4):

$$K_{root}(z_i) = K_{SL} \cdot \hat{U}_P(z_i). \tag{5}$$

Supporting Information: Appendix 1 also provides a more detailed discussion in Supporting Information: Figure 3 and the resulting conclusions.

2.5 | Determining the distribution of root length and root conductivity

Before and after the SWaP measurement, root length profiles of the plants were determined noninvasively using MRI. The MRI setup consisted of a 4.7 T vertical wide bore (310 mm) magnet (Magnex) and a gradient coil (ID 205 mm; MR Solutions) generating gradients up to 400 mT/m, controlled with an MR Solutions console. We used NMRooting software (van Dusschoten et al., 2016) to derive root length profiles at a vertical stepped-down resolution of 1 cm from the MRI data. To estimate the root length distribution at each intermediate day between the two MRI measurements, we applied an exponential interpolation in each layer separately, assuming exponential root growth during the 4 days. Since the MRI setup has a detection limit of roots with diameter around 200–300 µm we used correction factors to account for the distribution of fine roots. These correction factors were derived in a previous experiment comparing root length profiles measured with MRI and with scanning of harvested roots (Müllers, Postma, Poorter, Kochs, et al., 2022). Plants in that study and the present study were of the same age and grown under similar conditions until the onset of water stress. Root length profiles ($L(z_i)$) were used to determine how the intrinsic root hydraulic conductivity (conductance per root length, k_{root}) was distributed along the root system:

$$k_{root}(z_i) = \frac{K_{root}(z_i)}{L(z_i)}. \tag{6}$$

In layers with both, small conductance and small root length this calculation can lead to erratic results. Therefore, for determination of k_{root}, we neglected soil layers with few roots (root length <1 cm) or root conductance <0.001 $\text{mL}^{-1}\,\text{h}\,\text{MPa}^{-1}$.

2.6 | Statistical analysis

Generally, for data analysis of a certain parameter X, we considered its median value ($\tilde{X}$) among replicates of each species. Variability within the data set is given as median absolute deviation (MAD):

$$MAD = \text{median}(|X_i - \tilde{X}|), \tag{7}$$

with X_i being the measured values from each individual replicate. For each species separately, we used Wilcoxon sign tests (matched pairs) to test for statistically significant differences in each soil layer among the 4 different days. The tested null-hypothesis was that there are no significant differences among the 4 days. If not stated differently, significant differences refer to a p value of 0.05. To test for significant differences between species, we used Mann–Whitney U tests. Both, Wilcoxon tests and Mann–Whitney U tests were performed using the SciPy-package (Virtanen et al., 2020) in Python.

We used a log transformation of Equation (6) to quantify to what extent measured changes in K_{root} over time were associated with a change in root length and to what extent with a change in root conductivity:

$$\ln(K_{root}) = \ln(L) + \ln(k_{root}). \tag{8}$$

Following the approach described by Poorter and Nagel (2000), the relative contribution of a change in L to a change in K_{root} (C_L) was calculated as:

$$C_L = \frac{\Delta \ln(K_{root})}{\Delta \ln(L)}. \tag{9}$$

In Equation (9), the difference Δ refers to the measured differences between two points in time. The relative contribution of a change in k_{root} (C_k) is then given as:

$$C_k = 1 - C_L. \tag{10}$$

3 | RESULTS

Withholding water for 4 days resulted in a progressive, significant reduction in both the soil water content ($\bar{\theta}$) and soil water potential ($\bar{\Psi}_{soil}$) averaged over depth (Table 3). For both species, $\bar{\theta}$ decreased from 16 mL cm^{-3} at Day 1 to 8 mL cm^{-3} at Day 4. $\bar{\Psi}_{soil}$ decreased from −0.01 MPa at Day 1 to −0.09 MPa (faba bean), and −0.07 MPa (maize) respectively, at Day 4.

TABLE 3 Volumetric soil water content and soil water potential averaged over depth and across each day of the experiment.

Day	Faba bean $\bar{\theta}$ (%)	 $\bar{\Psi}_{soil}$ (MPa)	Maize $\bar{\theta}$ (%)	 $\bar{\Psi}_{soil}$ (MPa)
1	16.1 ± 2.0^a	-0.01 ± 0.00^a	16.0 ± 2.0^a	-0.01 ± 0.00^a
2	12.9 ± 1.2^b	-0.03 ± 0.01^b	13.4 ± 2.5^b	-0.02 ± 0.01^b
3	9.9 ± 1.2^c	-0.06 ± 0.01^c	10.7 ± 2.0^c	-0.04 ± 0.01^c
4	8.0 ± 1.2^d	-0.09 ± 0.03^d	7.8 ± 1.9^d	-0.07 ± 0.03^d

Note: Values are species medians with median absolute deviation. For each species separately, we tested for significant changes of each parameter among the 4 days using Wilcoxon rank tests. Different letters indicate significantly different values ($p < 0.05$).

Figure 2 shows how these reductions were distributed over depth. At Day 1 after withholding water, for both species, there was a vertical gradient in θ with drier soil layers in the top and wetter layers in the bottom (Figure 2a,c). θ ranged from 12 mL cm^{-3} (at 5 cm depth) to 20 mL cm^{-3} (44 cm) for faba bean and from 12 mL cm^{-3} (6 cm) to 23 mL cm^{-3} (44 cm) for maize (Table 4). In each individual soil layer, θ was significantly ($p < 0.01$) reduced from each day towards the next one for both species. At Day 4, θ ranged from 5 mL cm^{-3} (7 cm) to 11 mL cm^{-3} (38) cm for faba bean and from 5 mL cm^{-3} (5 cm) to 10 mL cm^{-3} (38 cm) for maize. Like θ, Ψ_{soil} in each individual soil layer decreased significantly ($p < 0.01$) from each to the next day for both species (Figure 2b,d). At Day 1, Ψ_{soil} was almost uniformly distributed, with only a slight vertical gradient (around −0.02 MPa in the upper half of the pot, and −0.01 MPa in the lower half for both species). However, proceeding soil drying led to an increase in the vertical gradient: At Day 4, Ψ_{soil} ranged from −0.23 MPa (at 7 cm depth) to −0.03 MPa (38 cm) for faba bean, and from −0.14 MPa (5 cm) to −0.04 MPa (38 cm) for maize. In conclusion, although the vertical gradient in θ even decreased during soil drying, the gradient in Ψ_{soil} increased strongly. This is due to the nonlinear character of the water retention curve: in the dry regime, a small reduction in θ causes a strong reduction in Ψ_{soil}.

In the next step, we analyzed how the changes in Ψ_{soil} affected root water uptake patterns measured as the normalized plant-driven root water uptake distributions ($\hat{U}_P$), using the SWaP. At Day 1, for both species there was a vertical gradient in $\hat{U}_P$ with greater values in upper soil layers and lower values in deeper layers (Figure 3). $\hat{U}_P$ was not constant over time: Generally, $\hat{U}_P$ decreased in the drier, upper soil layers, while it increased in relatively wetter, deeper layers. For the parameters described below, in deeper layers we observed a consistent trend from Days 1 to 3, reversing from Days 3 to 4. Therefore, we primarily tested for significant differences between Days 1 and 3. As indicated by a different background colour in Figure 3, we observed the following significant changes: For faba bean, $\hat{U}_P$ decreased in the top 8 cm ($p < 0.01$) and increased between 11 and 38 cm depth ($p < 0.05$ at 11–13 cm depth, <0.01 at 13–38 cm depth). For maize, $\hat{U}_P$ decreased in the top 10 cm ($p < 0.05$ at 10 cm depth, <0.001 else) and increased below 20 cm depth ($p < 0.05$ at 20–23 cm depth, <0.01 below).

Alterations of $\hat{U}_P$ are caused by a shift in the distribution of root hydraulic conductance (K_{root}). To derive the distribution of K_{root} over depth, we multiplied the daily average of the total conductance, as determined in a previous study (Müllers, Postma, Poorter, & van Dusschoten, 2022) (Table 2), with the daily $\hat{U}_P(z)$, according to

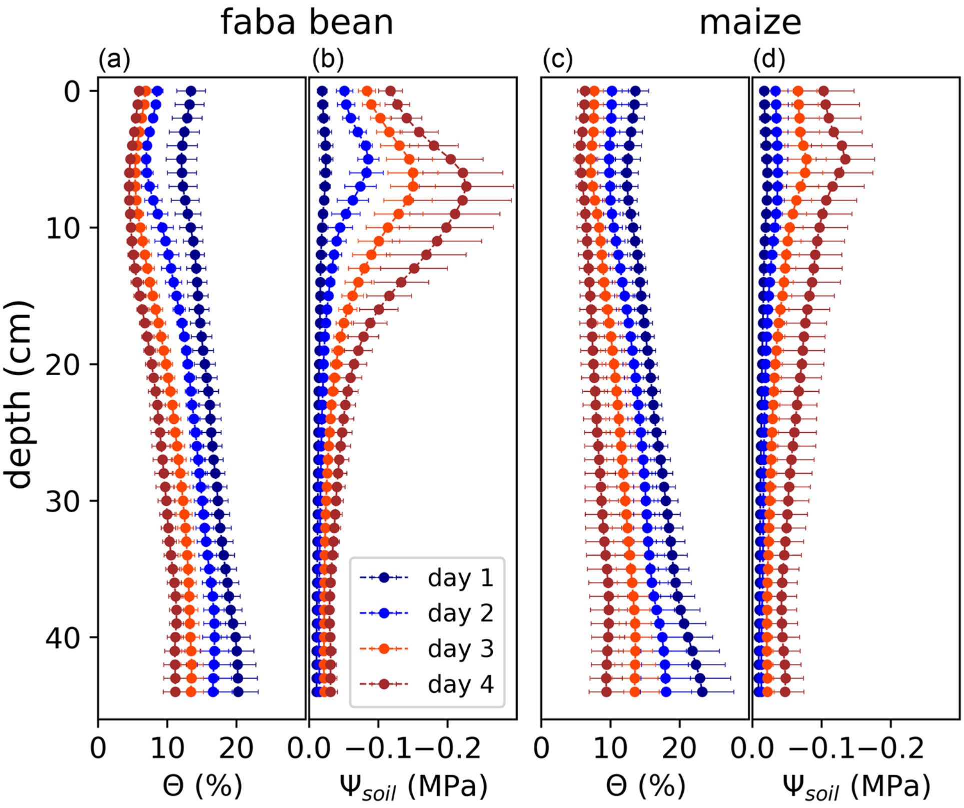

FIGURE 2 Distribution of soil moisture parameters over depth during 4 days of soil drying. (a and c) Show volumetric soil water content (θ), (b and d) show soil water potential (Ψ_{soil}). Data points are median values among all faba bean (a and c) and maize (b and d) replicates ($N = 10$). Error bars are median absolute deviations. A Wilcoxon rank test was used to test for significant differences among the 4 days of soil drying at each depth separately. In each soil layer, both, θ and Ψ_{soil}, decreased significantly between each of the 4 days.

TABLE 4 Maximal and minimal values of soil water content and soil water potential over depth, at each day of the measurement.

	Faba bean		Maize	
Day	$\theta_{\min}$ (%)	$\theta_{\max}$ (%)	$\theta_{\min}$ (%)	$\theta_{\max}$ (%)
1	12.0 ± 3.1^{a}	20.3 ± 4.0^{a}	12.4 ± 2.1^{a}	23.3 ± 6.8^{a}
2	6.9 ± 1.2^{b}	16.8 ± 3.2^{b}	9.7 ± 2.9^{b}	18.0 ± 5.1^{b}
3	5.4 ± 0.7^{c}	13.9 ± 1.7^{c}	6.8 ± 1.9^{c}	13.7 ± 4.3^{c}
4	4.5 ± 0.7^{d}	11.4 ± 2.0^{d}	5.4 ± 1.6^{d}	9.8 ± 3.1^{d}
	Faba bean		Maize	
Day	$\Psi_{\text{soil, min}}$ (MPa)	$\Psi_{\text{soil, max}}$ (MPa)	$\Psi_{\text{soil, min}}$ (MPa)	$\Psi_{\text{soil, max}}$ (MPa)
1	-0.02 ± 0.01^{a}	-0.01 ± 0.00^{a}	-0.02 ± 0.01^{a}	-0.01 ± 0.00^{a}
2	-0.09 ± 0.03^{b}	-0.01 ± 0.00^{b}	-0.04 ± 0.02^{b}	-0.01 ± 0.01^{b}
3	-0.15 ± 0.05^{c}	-0.02 ± 0.00^{c}	-0.09 ± 0.05^{c}	-0.02 ± 0.01^{c}
4	-0.23 ± 0.08^{d}	-0.03 ± 0.01^{d}	-0.14 ± 0.10^{d}	-0.04 ± 0.03^{d}

Note: Values are species medians with median absolute deviation. For each species separately, we tested for significant changes of each parameter among the 4 days using Wilcoxon rank tests. Different letters indicate significantly different values ($p < 0.05$).

Equation (5). The total conductance at the 1st day was similar for faba bean and maize (8–9 mL h^{-1} MPa^{-1} Table 2). At Day 1, for both species, there was a vertical gradient in K_{root} with greater values in upper soil layers (54% in the upper 10 cm for faba bean, 47% for maize) and lower values in the bottom (13% in the bottom half for faba bean, 21% for maize) (Figure 4). Withholding water for 4 days resulted in a strong reduction of K_{root} in upper soil layers with more negative Ψ_{soil}: For faba bean, K_{root} significantly decreased from

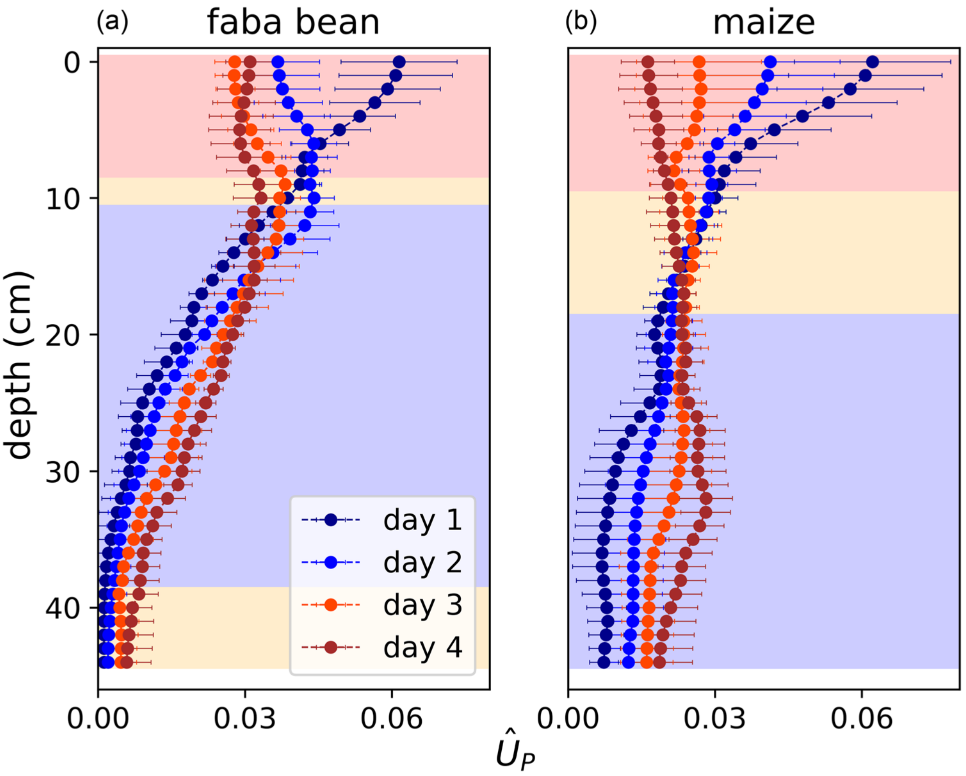

FIGURE 3 Normalized plant-driven root water uptake distribution ($\hat{U}_{\text{P}}$) over depth during 4 days of soil drying. Data points are median values among all faba bean (a) and maize (b) replicates ($N = 10$). Error bars are median absolute deviations. Background colour in each layer indicates a significant decrease (pink), increase (blue), or no significant change (yellow) between Days 1 and 3, tested with a Wilcoxon rank test. Days 1 and 3 were chosen as reference points, because the parameters analyzed below showed a consistent trend within this period.

Days 1 to 3 in the entire upper half of the pot ($p < 0.01$) by, on average, 72% (Figure 4a). In the lower half, K_{root} did not change significantly. For maize, K_{root} significantly decreased from Days 1 to 3 in the upper 16 cm of the pot ($p < 0.01$ above 12 cm depth, <0.05 else) by, on average, 66% (Figure 4b). However, between a depth of 31 and 41 cm, K_{root} increased significantly ($p < 0.01$ at 35–37 cm depth, <0.05 else) by, on average, 107% (Figure 4c). With proceeding soil drying from Days 3 to 4, K_{root} decreased again in these layers, such that it was not significantly different compared with Day 1.

The temporarily increased K_{root} in deeper parts of the maize root systems supports the uptake of deep soil water resources. We estimated the relevance of this facilitated deep water uptake by calculating how much it contributed to the total root water uptake (Figure 5). For maize, the measured increases in K_{root} contributed 5% to the total root water uptake rate at Day 2, 11% at Day 3, and 21% at Day 4. In different words, without the enhanced K_{root}, only 80% of the measured water uptake rate might have been realized at Day 4. Note that the hypothetical uptake rates (grey bars in Figure 5) were calculated by setting all measured increases in K_{root} to zero and assuming that this would not affect the leaf water potential, implying a strict stomatal control of the plant water status. More realistically, a lack of the increases in K_{root} would not be fully reflected in a reduction in total water uptake rate, but also partially in leaf water potential. However, mitigation of both, the drop in total root water uptake rate and in leaf water potential comes with reduced plant water stress. For faba bean, measured increases in K_{root} at each day contributed significantly less to the total root water uptake rate compared with maize ($p < 0.05$).

The determination of K_{root}, along with the associated increases in deeper layers for maize (Figures 4 and 5), are based on a correct separation of U_{P} and U_{S} by the SWaP measurements (Equations 1–3). Otherwise, the local increases might also be explained by an altered soil water distribution and the resulting compensated root water uptake. Although theoretically, U_{P} and U_{S} were separated using the fluctuating light intensity, we evaluated the potential effect of compensated root water uptake on U_{P} by comparing the changes in U_{P} and U_{S} between Days 1 and 3 in deeper layers for maize (Supporting Information: Appendix 2 and Figure 4). Below 20 cm depth, the measured U_{P} increased between Days 1 and 3 (Supporting Information: Figure 4A,D). Below 30 cm depth, this increase was of the order of 0.2 mL h^{-1} (Supporting Information: Figure 4C,F). At the same time, the estimated U_{S} also increased in these layers (Supporting Information: Figure 4B,E) indicating enhanced compensated root water uptake. However, U_{S} at Day 3 was only of the order of 0.02 m h^{-1}, and thus a factor 10 smaller than the increase in U_{P}. Calculation of U_{S} assuming no local increases in K_{root} (U_{S}', see Supporting Information: Appendix 2) gave even smaller values (Supporting Information: Figure 4B,E). In conclusion, even if U_{P} and

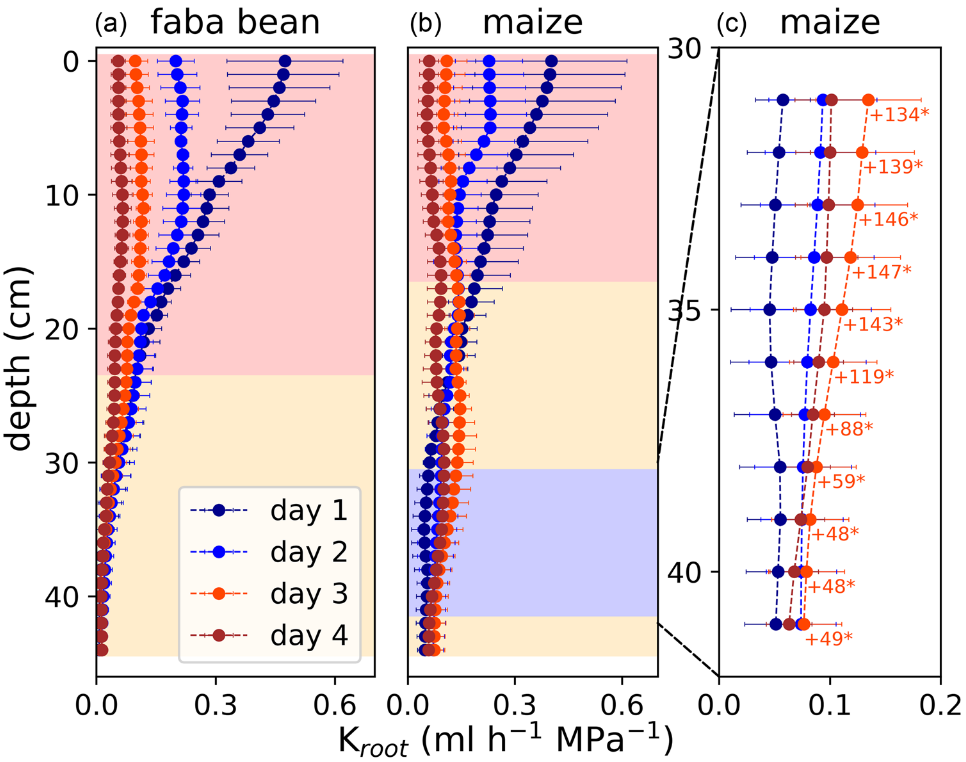

FIGURE 4 Distribution of root conductance (K_{root}) over depth during 4 days of soil drying. Data points are median values among all faba bean (a) and maize (b) replicates ($N = 10$). Error bars are median absolute deviations. Significant differences between Days 1 and 3 in each layer are indicated by the background colour, analogue to Figure 3. (c) Shows a magnification of (b) for layers with a significantly increasing K_{root} between Days 1 and 3. Values next to data points are percentage increases compared with Day 1.

U_S were not separated correctly by our approach, contribution of U_S to the increased U_P in deeper layers was marginal, such that the increase in K_{root} (Figures 4 and 5) remained.

We analyzed whether the locally enhanced K_{root} in maize was caused by additional root growth or an increase in root conductivity (conductance per length, k_{root}). Root length distributions at each day were derived from MRI images before and after the 4 days, making use of exponentially interpolating the data (Figure 6a–c). Then we derived k_{root} profiles at each day by dividing K_{root} by the root length distributions (Figure 6d–f). Initially, faba bean roots had a much greater conductivity (0.19 mL h^{-1} MPa^{-1} m^{-1} on average over depth) than maize roots (0.05 mL h^{-1} MPa^{-1} m^{-1} on average over depth). Like for the other parameters analyzed above, at Day 1, there was a vertical gradient in k_{root}. Shallow roots of both species had a greater conductivity than deeper roots. Withholding water for 4 days resulted in a decreasing k_{root} of shallow roots, in the faster drying, upper soil layers. In faba bean, k_{root} decreased significantly from Days 1 to 3 in the upper 29 cm of the pot ($p < 0.01$) by, on average, 76% (Figure 6d). Below 30 cm, k_{root} remained mostly constant. In maize, k_{root} decreased significantly from Days 1 to 3 in the upper 15 cm of the pot ($p < 0.01$ above 12 cm depth, <0.05 else) by, on average, 66% (Figure 6e). Between a depth of 27 and 35 cm, however, k_{root} increased significantly ($p < 0.05$) by up to 81% (Figure 6f). Like K_{root}, k_{root} from Days 3 to 4 decreased again in these layers. Distributions of k_{root} for each individual maize plant during the 4 days are shown in Supporting Information: Figure 5. For each plant, there were local increases in k_{root}, indicated by green dots, during the 4 days. The depth and day at which these increases occurred, however, varied strongly among the different replicates, causing the limited significance observed in Figure 6e. Using Equations (8–10), we calculated how much changes in root length, and k_{root} contributed to the significantly increased K_{root} at 31–41 cm depth for maize (Table 5). In each of these soil layers, the increase in K_{root} was primarily caused by an increase in k_{root} (relative contribution >0.75 in 8 out of 10 layers). Note that in some layers, root length even decreased slightly, causing the negative values for the contribution of root length and values >1 for the contribution of root conductivity in Table 5.

4 | DISCUSSION

The spatial distributions of root hydraulic traits and how they are affected by soil drying has important implications for the plant water balance. The strong reduction of soil water potential in upper soil layers led to a significant reduction of the local root hydraulic conductance. In maize, this was partly compensated by an increased conductivity (conductance per length) in deep roots. This enabled plants to maintain an estimated 20% greater total water uptake rate compared with a scenario without local increases in root conductance.

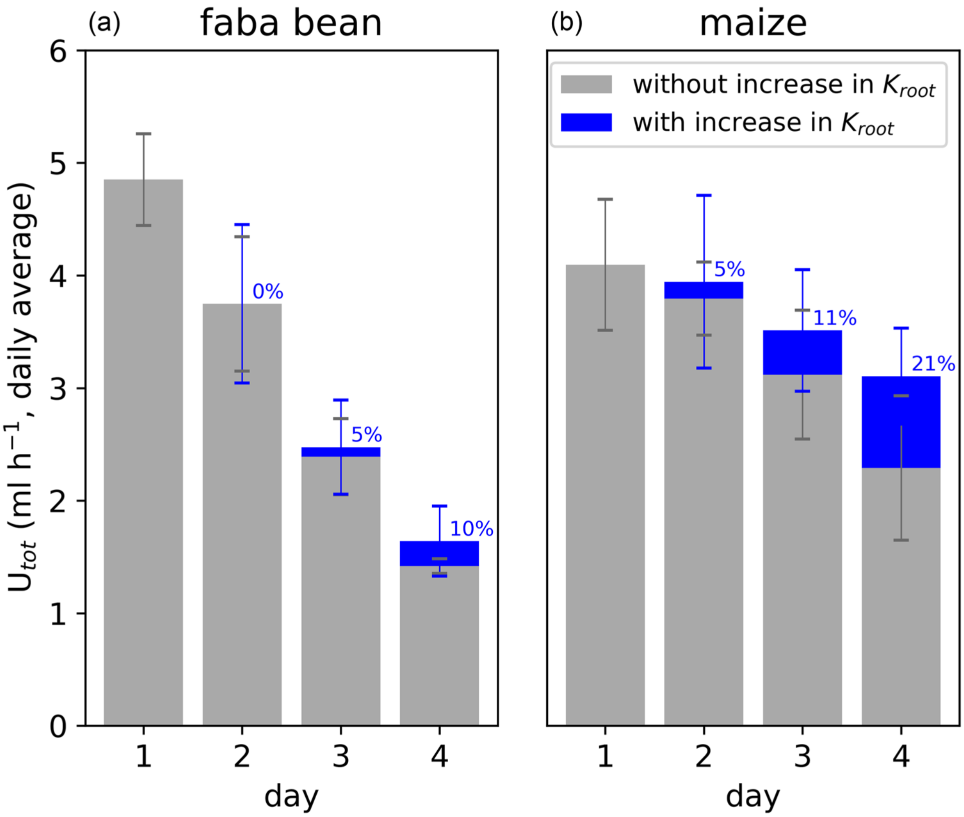

FIGURE 5 Effect of increases in root conductance on the total root water uptake rate (U_{tot}) during 4 days of soil drying. Grey bars are hypothetical uptake rates, calculated by setting all measured local increases in K_{root} to zero. Blue parts of the bars are the fractions of total water uptake rates attributed to the measured increases in K_{root}. Blue values give the relative contribution of these fractions to the measured uptake rates. Total water uptake rates are the temporal averages across the illuminated period at each day. Height of the error bars are medians among faba bean (a) and maize (b) replicates, error bars are median absolute deviations ($N = 10$).

Initially, root conductance in upper soil layers was much greater (87% in upper half of the pot for faba bean, 79% for maize) than in deeper soil layers (Figure 4). This is typical for well-watered conditions since shallow roots are usually more abundant (Haberle & Svoboda, 2015; Kemper et al., 2020; Righes, 1980) and more conductive than deeper roots (Dara et al., 2015; Müllers, Postma, Poorter, Kochs, et al., 2022; Zarebanadkouki et al., 2013). Consequently, withholding water resulted in a considerable vertical gradient in soil water potential with more negative values in the top and less negative values in the bottom (Figure 2). In response to soil drying, we observed a significant decrease in K_{root} in upper, relatively dry soil layers for both species (Figure 4). One plausible reason for this decrease is a partial loss of soil root contact due to root shrinkage, which was shown to be initiated at a soil water potential of around −0.02 MPa for faba bean (Koebernick et al., 2018) and maize (Duddek et al., 2022). Therefore, in upper soil layers, the relatively low (more negative) Ψ_{soil} might have induced root shrinkage in our study, resulting in the observed reduction in K_{root}, whereas in deeper layers, Ψ_{soil} was still sufficiently high (less negative). Nevertheless, the critical Ψ_{soil} at which we observed significant reductions in K_{root} was around −0.04 MPa (compare Figures 2 and 4), and thus slightly more negative than reported by the two studies mentioned above. Besides a loss of soil-root contact, K_{root} can also decrease due to enhanced root suberization and reducing the amount of active aquaporins, two mechanisms which are under biological control of the plant. Soil drying reportedly led to a decreased expression of aquaporin genes in shallow roots (Johnson et al., 2014), and an enhanced suberization of, especially, basal root parts (Kreszies et al., 2019) which predominantly reside in the top soil. Both processes might have contributed to the observed reduction in K_{root} in upper soil layers (Figure 4).

We assumed that the soil conductance was much greater than the root conductance to approximate K_{root} by K_{SL} (Equations 4 and 5). Estimations of K_{soil} (Supporting Information: Appendix 1) showed that this approximation was justified for a large part of the measurement (Supporting Information: Figure 3). Only in upper soil layers for faba bean at Day 4, K_{soil} was of the same order of magnitude as K_{root} (Supporting Information: Figure 3I). There, up to 8% of the decline in K_{root} from Days 3 to 4 as shown in Figure 4 were caused by a reduction in K_{soil}. Nevertheless, this effect was of minor importance, as K_{root} was already reduced by 72% on average between Days 1 and 3 in the upper half of the pot.

Theoretically, unregulated water uptake from drying soils can lead to steep water potential gradients in the soil around roots and

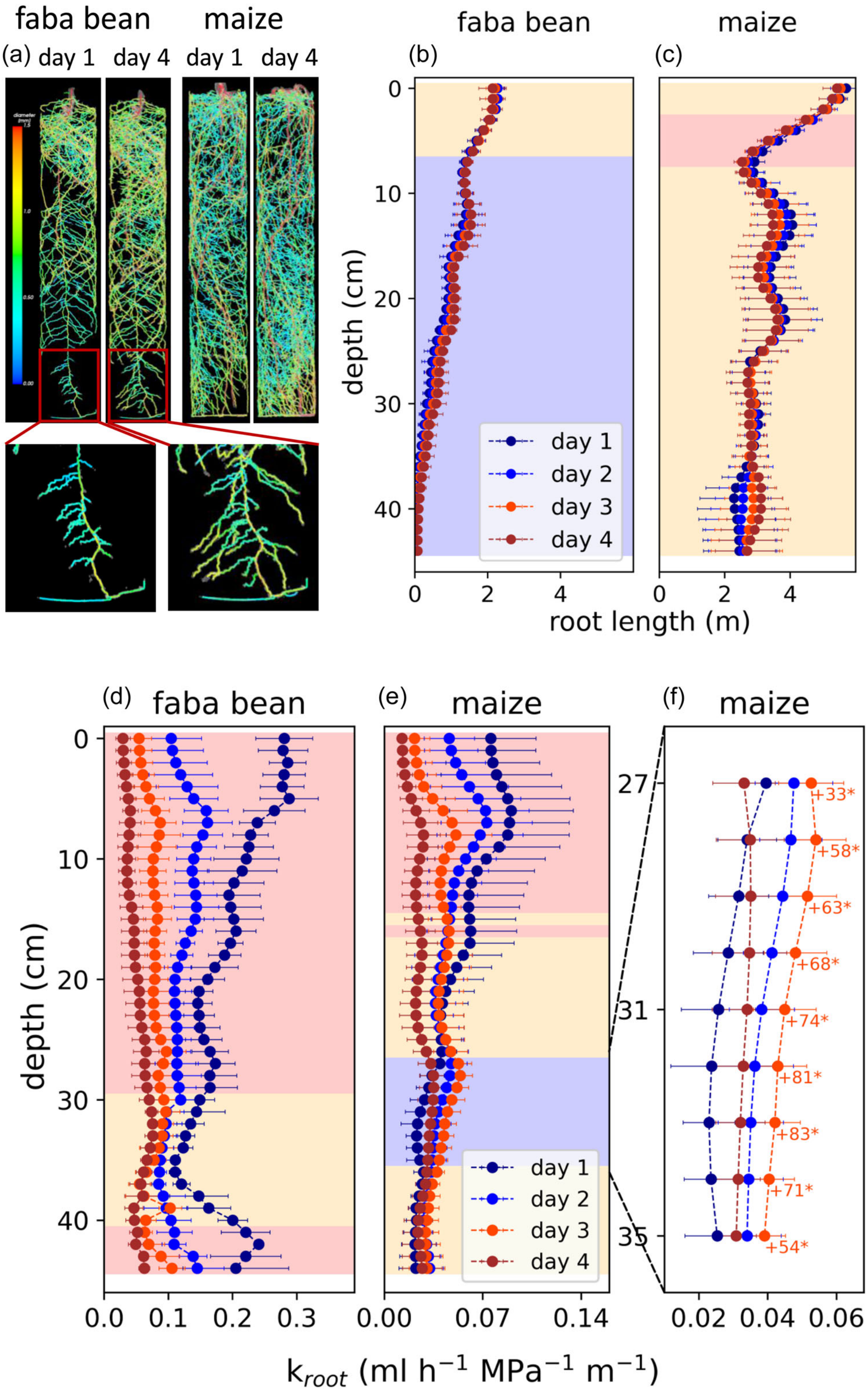

FIGURE 6 Distribution of root length and root conductivity (conductance per root length, k_{root}) over depth during 4 days of soil drying. Example, MRI images show the root system of a faba bean and maize plant at the first and last day of the measurement (a). Pseudo colours indicate root diameter with the colour bar ranging from 0 mm (blue) to 1.5 mm (red). Root length distribution over depth for faba bean (b) and maize (c) were derived from the MRI images. Data points are median values, error bars are median absolute deviations. Significant differences between Days 1 and 4 in each layer are indicated by the background colour, analogue to Figure 3. The distributions of k_{root} over depth (d and e) were derived by dividing K_{root} as shown in Figure 4 by the root length distributions. (f) Shows a magnification of (e) for layers with a significantly increasing k_{root} between Days 1 and 3. Values next to data points are percentage changes compared with Day 1.

TABLE 5 Contribution of changes in root length and conductivity to the significant increase in maize root conductance between Days 1 and 3 at 31–41 cm depth as shown in Figure 4c.

Depth (cm)	Relative contribution root length	Relative contribution conductivity
31	−0.09 ± 0.31	1.09 ± 0.31
32	−0.05 ± 0.39	1.05 ± 0.39
33	−0.02 ± 0.48	1.02 ± 0.48
34	−0.00 ± 0.49	1.00 ± 0.49
35	0.08 ± 0.45	0.92 ± 0.45
36	0.38 ± 0.40	0.62 ± 0.40
37	0.41 ± 0.44	0.59 ± 0.44
38	0.22 ± 0.40	0.78 ± 0.40
39	0.15 ± 0.50	0.85 ± 0.50
40	0.20 ± 0.54	0.80 ± 0.54
41	0.24 ± 0.56	0.76 ± 0.56

Note: Data were calculated using the log-transformed differences between Days 1 and 3. Values are median values with median absolute deviations. Values <0 for the contribution of root length (and >1 for the contribution of conductivity) are caused by a decrease in root length between the two points in time.

thus interrupt the hydraulic pathway from the bulk soil towards the roots, and force stomatal closure (Carminati & Javaux, 2020). Our estimations of the water potential at the root surface (Supporting Information: Figure 3A,C) emphasize that such a severe water depletion zone did not occur during the measurements presented here. Most likely, the early local reduction in K_{root}, due to the mechanisms discussed above, and the resulting stomatal closure, could prevent an incisive drop in the local K_{soil}. These conclusions on the effect of K_{soil} initially apply only to the soil type used in this study, a loamy sand. In this context, a recent study showed that the total conductance between soil and plant decreased at a less negative Ψ_{soil} in a sandy soil compared with loamy soil, probably because the loamy soil sustained a greater conductivity at a given Ψ_{soil} (Cai et al., 2022). Additionally, the effect of a reduced soil-root contact depends on soil texture, and might be more pronounced in the loamy sand used here, compared with a sandy soil (Carminati et al., 2009).

Despite the potential benefit of preventing a severe water depletion zone around the roots, the strong reduction in K_{root} in upper soil layers (76% reduction in faba bean, 66% reduction in maize [Figure 4]) comes with different impairments for the plant: A reduction in K_{root} hampers the hydraulic redistribution of soil water from relatively wetter towards relatively drier soil layers through the roots (Neumann & Cardon, 2012). Moreover, as demonstrated in a previous study, the reduction in K_{root} amplifies the drop in plant water potential (Müllers, Postma, Poorter, & van Dusschoten, 2022). One possibility to partly compensate for this is deep-water uptake. Up until Day 3, water in the bottom third of the pots was much easier to access (Ψ_{soil} less negative than −0.03 MPa) than water in shallow soil layers (Ψ_{soil} locally as low as −0.15 MPa [faba bean] and −0.08 MPa [maize] [Figure 2]). However, in agreement with other studies (Clément et al., 2022; Dara et al., 2015; Zarebanadkouki et al., 2013), effectively taking up deep water was initially limited by a low local K_{root} (Figure 4). With proceeding soil drying, maize, but not faba bean was able to significantly increase K_{root} in deeper, comparably wet soil layers. The deep-water uptake, facilitated in this way, contributed up to 20% to the total root water uptake rate in maize (Figure 5) and thus, at least temporarily, alleviated the drop in plant water potential.

Deep-water uptake under drought can increase due to a local increase in root conductance, but also due to compensated root water uptake, quantified as U_S. This happens when the local Ψ_{soil} drops less than the global Ψ_{seq} which was the case in deeper soil layers in our study (compare Figure 2 and Table 2). Theoretically, we had separated U_P and U_S using the fluctuating light intensity which, on short time scales, only changes U_P but not U_S. To not fully rely on the success of this separation, we additionally estimated which impact it had for our conclusions on K_{root} if compensated water uptake had influenced the measured U_P (Supporting Information: Appendix 2). Since the estimated U_S at Day 3 in deeper layers in maize was a factor 10 smaller than the measured increase in U_P (Supporting Information: Figure 4), we conclude that the measured local increases in K_{root} largely remained, even if the separation of U_P and U_S had failed.

Normalization by root length indicated that the increase in K_{root} was mainly caused by a significantly increased root conductivity (conductance per length) (Figure 6). One potential reason for this phenomenon is directed, enhanced aquaporin gene expression, as observed by Johnson et al. (2014) or McLean et al. (2011). By relating empirical data on Ψ_{soil}, ABA concentration in roots, and its impact on aquaporin expression, Couvreur et al. (2015) estimated a 250% increase in k_{root} between a local Ψ_{soil} of −0.005 and −0.1 MPa. This effect would lead to a net increase in k_{root} as long as it is not outweighed by a reduced soil-root contact and other forementioned processes reducing k_{root}. The fact that increases in k_{root} only occurred above a Ψ_{soil} of −0.04 MPa in our study (compare Figures 2 and 6e,f) fits these considerations. Furthermore, the different abilities of faba bean and maize to increase K_{root} might be explained by root aquaporin regulation as well: Under nonstressed conditions, radial water uptake in bean occurs predominantly via the cell-to-cell pathway, mediated by aquaporins, whereas in maize, the apoplastic pathway contributes considerably (Javot & Maurel, 2002; Steudle & Brinckmann, 1989; Steudle & Frensch, 1989). This fits the initially greater conductivity of faba bean roots compared to maize roots (Figure 6a,b at Day 1). To compensate this, maize had a greater root length (Figure 6b,c), thus achieving a similar initial conductance (compare Figure 4a and 4b at Day 1) with a greater flexibility and potential for local increases via a facilitated cell-to-cell water transport.

However, the observed increase in k_{root} could have also been caused by xylem maturation. As summarized by M. McCully (1995), maturation of the late metaxylem can occur far behind the root tip (up to 10–50 cm) for various species, including maize (St. Aubin et al., 1986) and soybean (M.E. McCully, 1994). Since maturation of the metaxylem results in an increase in axial conductivity, the measured increase in k_{root} in maize possibly reflects the development of xylem vessels. This would imply that the axial conductivity had initially limited root water uptake in deeper soil layers, as suggested by previous studies (Clément et al., 2022; Sanderson et al., 1988; Strock et al., 2021). However, the strong increase in local k_{root} (up to 82%) indicates a simultaneous response of all roots of various growth stages within the respective soil layers, rather than a continuous developmental process. Additionally, Steudle & Peterson (1998) reported for maize that even though the late metaxylem is not fully developed within 25 cm from the root tip, axial conductance is orders of magnitude greater than radial conductance, except for a small apical region without developed early metaxylem. We conclude that an increased amount of active aquaporins is a plausible explanation for the measured local increases in k_{root}, which could have been enhanced by other mechanisms, such as xylem development.

5 | CONCLUSION

We analyzed the effect of soil drying on vertical profiles of root hydraulic conductance in faba bean and maize. Withholding water for 4 days resulted in a pronounced vertical gradient in soil water potential with drier layers in the top and wetter layers in the bottom. In drier, shallow soil layers, the reduced soil water potential caused a strong decrease in root conductance, which on the one hand prevented a severe drop in soil hydraulic conductivity around the roots, on the other hand amplified water stress and forced stomatal closure. To partly compensate for this, maize, in contrast to faba bean, was able to facilitate deep water uptake by locally increasing its root conductivity. This increase improved the overall water uptake rate, and thus is an effective plant strategy to reduce water stress during soil drying.

ACKNOWLEDGEMENTS

This study was institutionally funded by the Helmholtz Association, Germany – POF4-899. Open access was partly funded by the Deutsche Forschungsgemeinschaft (DFG, German Research Foundation) – 491111487. Open Access funding enabled and organized by Projekt DEAL.

DATA AVAILABILITY STATEMENT

The data are available on request from the corresponding author, Dagmar van Dusschoten.

ORCID

Yannik Müllers http://orcid.org/0000-0002-0475-3734
Johannes A. Postma http://orcid.org/0000-0002-5222-6648

REFERENCES

Ahmed, M.A., Zarebanadkouki, M., Kaestner, A. & Carminati, A. (2016) Measurements of water uptake of maize roots: the key function of lateral roots. *Plant and Soil*, 398(1–2), 59–77. Available at: https://doi.org/10.1007/s11104-015-2639-6

Ahmed, M.A., Zarebanadkouki, M., Meunier, F., Javaux, M., Kaestner, A. & Carminati, A. (2018) Root type matters: measurement of water uptake by seminal, crown, and lateral roots in maize. *Journal of Experimental Botany*, 69(5), 1199–1206. https://doi.org/10.1093/jxb/erx439

Alsina, M.M., Smart, D.R., Bauerle, T., De Herralde, F., Biel, C., Stockert, C. et al. (2011) Seasonal changes of whole root system conductance by a drought-tolerant grape root system. *Journal of Experimental Botany*, 62(1), 99–109. https://doi.org/10.1093/jxb/erq247

Asseng, S., Ritchie, J.T., Smucker, A.J.M. & Robertson, M.J. (1998) Root growth and water uptake during water deficit and recovering in wheat. *Plant and Soil*, 201(2), 265–273. https://doi.org/10.1023/A:1004317523264

Barrios-Masias, F.H., Knipfer, T. & McElrone, A.J. (2015) Differential responses of grapevine rootstocks to water stress are associated with adjustments in fine root hydraulic physiology and suberization. *Journal of Experimental Botany*, 66(19), 6069–6078. https://doi.org/10.1093/jxb/erv324

Bartlett, M.K., Scoffoni, C. & Sack, L. (2012) The determinants of leaf turgor loss point and prediction of drought tolerance of species and biomes: a global meta-analysis. *Ecology Letters*, 15(5), 393–405. https://doi.org/10.1111/j.1461-0248.2012.01751.x

Bourbia, I., Pritzkow, C. & Brodribb, T.J. (2021) Herb and conifer roots show similar high sensitivity to water deficit. *Plant Physiology*, 186(4), 1908–1918. https://doi.org/10.1093/PLPHYS/KIAB207

Cai, G., König, M., Carminati, A., Abdalla, M., Javaux, M. & Wankmüller, F. et al. (2022) Transpiration response to soil drying and vapor pressure deficit is soil texture specific. *Plant and Soil* 17. https://doi.org/10.1007/s11104-022-05818-2

Carminati, A. & Javaux, M. (2020) Soil rather than xylem vulnerability controls stomatal response to drought. *Trends in Plant Science*, 25(9), 868–880. https://doi.org/10.1016/j.tplants.2020.04.003

Carminati, A., Vetterlein, D., Weller, U., Vogel, H.-J. & Oswald, S.E. (2009) When roots lose contact. *Vadose Zone Journal*, 8(3), 805–809. https://doi.org/10.2136/vzj2008.0147

Clément, C., Schneider, H.M., Dresbøll, D.B., Lynch, J.P. & Thorup-Kristensen, K. (2022) Root and xylem anatomy varies with root length, root order, soil depth and environment in intermediate wheatgrass (Kernza®) and alfalfa. *Annals of Botany*, 130, 367–382. https://doi.org/10.1093/aob/mcac058

Cochard, H. (2002) Xylem embolism and drought-induced stomatal closure in maize. *Planta*, 215(3), 466–471. https://doi.org/10.1007/s00425-002-0766-9

Corso, D., Delzon, S., Lamarque, L.J., Cochard, H., Torres-Ruiz, J.M., King, A. et al. (2020) Neither xylem collapse, cavitation, or changing leaf conductance drive stomatal closure in wheat. *Plant, Cell & Environment*, 43(4), 854–865. https://doi.org/10.1111/pce.13722

Couvreur, V., Vanderborght, J., Draye, X. & Javaux1, M. (2015) Dynamic aspects of soil water availability for isohydric plants: focus on root hydraulic resistances. *Water Resources Research*, 51, 2707–2723. https://doi.org/10.1002/2014WR015608.Received

Couvreur, V., Vanderborght, J. & Javaux, M. (2012) A simple three-dimensional macroscopic root water uptake model based on the hydraulic architecture approach. *Hydrology and Earth System Sciences*, 16(8), 2957–2971. https://doi.org/10.5194/hess-16-2957-2012

Cruz, R.T., Jordan, W.R. & Drew, M.C. (1992) Structural changes and associated reduction of hydraulic conductance in roots of *Sorghum bicolor* L. following exposure to water deficit. *Plant Physiology*, 99(1), 203–212. https://doi.org/10.1104/pp.99.1.203

Dara, A., Moradi, B.A., Vontobel, P. & Oswald, S.E. (2015) Mapping compensating root water uptake in heterogeneous soil conditions via neutron radiography. *Plant and Soil*, 397(1–2), 273–287. https://doi.org/10.1007/s11104-015-2613-3

Dubrovsky, J.G., North, G.B. & Nobel, P.S. (1998) Root growth, developmental changes in the apex, and hydraulic conductivity for Opuntia ficus-indica during drought. *New Phytologist*, 138(1), 75–82. https://doi.org/10.1046/j.1469-8137.1998.00884.x

Duddek, P., Carminati, A., Koebernick, N., Ohmann, L., Lovric, G., Delzon, S. et al. (2022) The impact of drought-induced root and root hair shrinkage on root–soil contact. *Plant Physiology*, 189, 1232–1236. https://doi.org/10.1093/plphys/kiac144

van Dusschoten, D., Kochs, J., Kuppe, C.W., Sydoruk, V.A., Couvreur, V., Pflugfelder, D. et al. (2020) Spatially resolved root water uptake determination using a precise soil water sensor. *Plant Physiology*, 184(3), 1221–1235. https://doi.org/10.1104/pp.20.00488

van Dusschoten, D., Metzner, R., Kochs, J., Postma, J.A., Pflugfelder, D. & Buehler, J. et al. (2016) Quantitative 3D analysis of plant roots growing in soil using magnetic resonance imaging. *Plant Physiology*, 170(3), 1176–1188. https://doi.org/10.1104/pp.15.01388

Frensch, J. & Steudle, E. (1989). Axial and radial hydraulic resistance to roots of maize (*Zea mays* L.). *Plant Physiology*, 91(2), 719–726. https://doi.org/10.1104/pp.91.2.719

Gessler, A., Bächli, L., Rouholahnejad Freund, E., Treydte, K., Schaub, M., Haeni, M. et al. (2022) Drought reduces water uptake in beech from the drying topsoil, but no compensatory uptake occurs from deeper soil layers. *New Phytologist*, 233, 194–206. https://doi.org/10.1111/nph.17767

Haberle, J. & Svoboda, P. (2015) Calculation of available water supply in crop root zone and the water balance of crops. *Contributions to Geophysics and Geodesy*, 45(4), 285–298. https://doi.org/10.1515/congeo-2015-0025

Hillel, D., Talpaz, H. & Keulen, H.V. (1976) A macroscopic-scale model of water uptake by a nonuniform root system and of water and salt movement in the soil profile. *Soil Science*, 121(4), 242–255.

Hu, T., Kang, S., Li, F. & Zhang, J. (2011) Effects of partial root-zone irrigation on hydraulic conductivity in the soil-root system of maize plants. *Journal of Experimental Botany*, 62(12), 4163–4172. https://doi.org/10.1093/jxb/err110

Javot, H. (2002) The role of aquaporins in root water uptake. *Annals of Botany*, 90(3), 301–313. https://doi.org/10.1093/aob/mcf199

Johnson, D.M., Sherrard, M.E., Domec, J.C. & Jackson, R.B. (2014) Role of aquaporin activity in regulating deep and shallow root hydraulic conductance during extreme drought. *Trees*, 28(5), 1323–1331. https://doi.org/10.1007/s00468-014-1036-8

Kemper, R., Bublitz, T.A., Müller, P., Kautz, T., Döring, T.F. & Athmann, M. (2020) Vertical root distribution of different cover crops determined with the profile wall method. *Agriculture*, 10(11), 503. https://doi.org/10.3390/agriculture10110503

Koebernick, N., Schlüter, S., Blaser, S.R.G.A. & Vetterlein, D. (2018) Root-soil contact dynamics of *Vicia faba* in sand. *Plant and Soil*, 431, 417–431.

Kondo, M., Murty, M.V.R. & Aragones, D.V. (2000) Characteristics of root growth and water uptake from soil in upland rice and maize under water stress. *Soil Science and Plant Nutrition*, 46(3), 721–732. https://doi.org/10.1080/00380768.2000.10409137

Kreszies, T., Shellakkutti, N., Osthoff, A., Yu, P., Baldauf, J.A., Zeisler-Diehl, V.V. et al. (2019) Osmotic stress enhances suberization of apoplastic barriers in barley seminal roots: analysis of chemical, transcriptomic and physiological responses. *New Phytologist*, 221(1), 180–194. https://doi.org/10.1111/nph.15351

Li, Y., Sperry, J.S. & Shao, M. (2009) Hydraulic conductance and vulnerability to cavitation in corn (*Zea mays* L.) hybrids of differing drought resistance. *Environmental and Experimental Botany*, 66(2), 341–346. https://doi.org/10.1016/j.envexpbot.2009.02.001

Lo Gullo, M.A., Nardini, A., Salleo, S. & Tyree, M.T. (1998) Changes in root hydraulic conductance (K(R)) of Olea oleaster seedlings following drought stress and irrigation. *New Phytologist*, 140(1), 25–31. https://doi.org/10.1046/j.1469-8137.1998.00258.x

Markesteijn, L., Iraipi, J., Bongers, F. & Poorter, L. (2010) Seasonal variation in soil and plant water potentials in a Bolivian tropical moist and dry forest. *Journal of Tropical Ecology*, 26(5), 497–508. https://doi.org/10.1017/S0266467410000271

Martre, P., North, G.B. & Nobel, P.S. (2001) Hydraulic conductance and mercury-sensitive water transport for roots of Opuntia acanthocarpa in relation to soil drying and rewetting. *Plant Physiology*, 126(1), 352–362. https://doi.org/10.1104/pp.126.1.352

McCully, M. (1995) How do real roots work? (Some new views of root structure). *Plant Physiology*, 109, 1–6. https://doi.org/10.1104/pp.109.1.1

McCully, M.E. (1994) Accumulation of high levels of potassium in the developing xylem elements in roots of soybean and some other dicotyledons. *Protoplasma*, 183(1–4), 116–125. https://doi.org/10.1007/BF01276819

McDowell, N.G. (2011) Mechanisms linking drought, hydraulics, carbon metabolism, and vegetation mortality. *Plant Physiology*, 155(3), 1051–1059. https://doi.org/10.1104/pp.110.170704

McLean, E.H., Ludwig, M. & Grierson, P.F. (2011) Root hydraulic conductance and aquaporin abundance respond rapidly to partial root-zone drying events in a riparian Melaleuca species. *New Phytologist*, 192(3), 664–675. https://doi.org/10.1111/j.1469-8137.2011.03834.x

Müllers, Y., Postma, J.A., Poorter, H. & van Dusschoten, D. (2022) Stomatal conductance tracks soil-to-leaf hydraulic conductance in faba bean and maize during soil drying. *Plant Physiology*, 190, 2279–2294. https://doi.org/10.1093/plphys/kiac422

Müllers, Y., Postma, J.A., Poorter, H., Kochs, J., Pflugfelder, D. & Schurr, U. et al. (2022) Shallow roots of different crops have greater water uptake rates per unit length than deep roots in well-watered soil. *Plant and Soil*, 481, 475–493. https://doi.org/10.1007/s11104-022-05650-8

Neumann, R.B. & Cardon, Z.G. (2012) The magnitude of hydraulic redistribution by plant roots: a review and synthesis of empirical and modeling studies. *New Phytologist*, 194(2), 337–352. https://doi.org/10.1111/j.1469-8137.2012.04088.x

Nobel, P.S. & Cui, M. (1992) Shrinkage of attached roots of opuntia ficus-indica in response to lowered water potentials—predicted consequences for water uptake or loss to soil. *Annals of Botany*, 70(6), 485–491. https://doi.org/10.1093/oxfordjournals.aob.a088508

North, G.B. & Nobel, P.S. (1991) Changes in hydraulic conductivity and anatomy caused by drying and rewetting roots of *Agave deserti* (Agavaceae). *American Journal of Botany*, 78(7), 906–915.

Passioura, J.B. (1983) Roots and drought resistance. *Agricultural Water Management*, 7(1–3), 265–280. https://doi.org/10.1016/0378-3774(83)90089-6

Pohlmeier, A., Haber-Pohlmeier, S. & Stapf, S. (2009) A fast field cycling nuclear magnetic resonance relaxometry study of natural soils. *Vadose Zone Journal*, 8(3), 735–742. https://doi.org/10.2136/vzj2008.0030

Poorter, H. & Nagel, O. (2000) The role of biomass allocation in the growth response of plants to different levels of light, CO_2, nutrients and water: a quantitative review. *Functional Plant Biology*, 27(6), 595–607. https://doi.org/10.1071/pp99173_co

Prechsl, U.E., Burri, S., Gilgen, A.K., Kahmen, A. & Buchmann, N. (2015) No shift to a deeper water uptake depth in response to summer drought of two lowland and sub-alpine C_3-grasslands in Switzerland. *Oecologia*, 177(1), 97–111. https://doi.org/10.1007/s00442-014-3092-6

Rasmussen, C.R., Thorup-Kristensen, K. & Dresbøll, D.B. (2020). Uptake of subsoil water below 2 m fails to alleviate drought response in deep-rooted Chicory (*Cichorium intybus* L.). *Plant and Soil*, 446(1–2), 275–290. https://doi.org/10.1007/s11104-019-04349-7

Reid, J.B. & Hutchison, B. (1986) Soil and plant resistances to water uptake by *Vicia faba* L. *Plant and Soil*, 92(3), 431–441. https://doi.org/10.1007/BF02372491

Rewald, B., Raveh, E., Gendler, T., Ephrath, J.E. & Rachmilevitch, S. (2012) Phenotypic plasticity and water flux rates of *Citrus* root orders under salinity. *Journal of Experimental Botany*, 63(7), 2717–2727. https://doi.org/10.1093/jxb/err457

Righes, A.A. (1980) Water uptake and root distribution of soybeans, grain sorghum and corn. *Retrospective Theses and Dissertations*. 134. https://lib.dr.iastate.edu/rtd/7122/

Rodrigues, M.L., Pacheco, C.M.A. & Chaves, M.M. (1995) Soil-plant water relations, root distribution and biomass partitioning in *Lupinus albus* L. under drought conditions. *Journal of Experimental Botany*, 46(8), 947–956. https://doi.org/10.1093/jxb/46.8.947

Rodriguez-Dominguez, C.M. & Brodribb, T.J. (2020) Declining root water transport drives stomatal closure in olive under moderate water stress. *New Phytologist*, 225(1), 126–134. https://doi.org/10.1111/nph.16177

Rodríguez-Gamir, J., Xue, J., Clearwater, M.J., Meason, D.F., Clinton, P.W. & Domec, J.C. (2019) Aquaporin regulation in roots controls plant hydraulic conductance, stomatal conductance, and leaf water potential in *Pinus radiata* under water stress. *Plant, Cell & Environment*, 42(2), 717–729. https://doi.org/10.1111/pce.13460

Ryu, J., Hwang, B.G., Kim, Y.X. & Lee, S.J. (2016) Direct observation of local xylem embolisms induced by soil drying in intact *Zea mays* leaves. *Journal of Experimental Botany*, 67(9), 2617–2626. https://doi.org/10.1093/jxb/erw087

Saliendra, N.Z. & Meinzer, F.C. (1989) Relationship between root/soil hydraulic properties and stomatal behavior in sugarcane. *Australian Journal of Plant Physiology*, 16(3), 241–250. https://doi.org/10.1071/PP9890241

Sanderson, J., Whitbread, F.C. & Clarkson, D.T. (1988) Persistent xylem cross-walls reduce the axial hydraulic conductivity in the apical 20 cm of barley seminal root axes: implications for the driving force for water movement. *Plant, Cell & Environment*, 11(4), 247–256. https://doi.org/10.1111/j.1365-3040.1988.tb01143.x

Sharp, R.E. & Davies, W.J. (1985) Root growth and water uptake by maize plants in drying soil. *Journal of Experimental Botany*, 36(9), 1441–1456. https://doi.org/10.1093/jxb/36.9.1441

St. Aubin, G., Canny, M.J. & Mccully, M.E. (1986) Living vessel elements in the late metaxylem of sheathed maize roots. *Annals of Botany*, 58(4), 577–588. https://doi.org/10.1093/annbot/58.4.577

Steudle, E. & Brinckmann, E. (1989) The osmometer model of the root: water and solute relations of roots of *Phaseolus coccineus*. *Botanica Acta*, 102(1), 85–95. https://doi.org/10.1111/j.1438-8677.1989.tb00071.x

Steudle, E. & Frensch, J. (1989) Osmotic responses of maize roots: water and solute relations. *Planta*, 177(3), 281–295. https://doi.org/10.1007/BF00403585

Steudle, E. & Peterson, C.A. (1998) How does water get through roots? *Journal of Experimental Botany*, 49(322), 775–788. https://doi.org/10.1093/jexbot/49.322.775

Strock, C.F., Burridge, J.D., Niemiec, M.D., Brown, K.M. & Lynch, J.P. (2021) Root metaxylem and architecture phenotypes integrate to regulate water use under drought stress. *Plant, Cell & Environment*, 44(1), 49–67. https://doi.org/10.1111/pce.13875

Thompson, M.V. (2006) Phloem: the long and the short of it. *Trends in Plant Science*, 11(1), 26–32. https://doi.org/10.1016/j.tplants.2005.11.009

Urli, M., Porte, A.J., Cochard, H., Guengant, Y., Burlett, R. & Delzon, S. (2013) Xylem embolism threshold for catastrophic hydraulic failure in angiosperm trees. *Tree Physiology*, 33(7), 672–683. https://doi.org/10.1093/treephys/tpt030

Virtanen, P., Gommers, R., Oliphant, T.E., Haberland, M., Reddy, T., Cournapeau, D. et al. (2020) SciPy 1.0: fundamental algorithms for scientific computing in Python. *Nature Methods*, 17(3), 261–272. https://doi.org/10.1038/s41592-019-0686-2

Wan, C., Sosebee, R.E. & McMichael, B.L. (1994) Hydraulic properties of shallow vs. deep lateral roots in a semiarid shrub, *Gutierrezia sarothrae*. *American Midland Naturalist*, 131(1), 120–127.

Wasson, A.P., Richards, R.A., Chatrath, R., Misra, S.C., Prasad, S.V.S., Rebetzke, G.J. et al. (2012) Traits and selection strategies to improve root systems and water uptake in water-limited wheat crops. *Journal of Experimental Botany*, 63(9), 3485–3498. https://doi.org/10.1093/jxb/ers111

Zarebanadkouki, M., Kim, Y.X. & Carminati, A. (2013) Where do roots take up water? Neutron radiography of water flow into the roots of transpiring plants growing in soil. *New Phytologist*, 199(4), 1034–1044. https://doi.org/10.1111/nph.12330

SUPPORTING INFORMATION

Additional supporting information can be found online in the Supporting Information section at the end of this article.

How to cite this article: Müllers, Y., Postma, J.A., Poorter, H. & Dusschoten, D. (2023) Deep-water uptake under drought improved due to locally increased root conductivity in maize, but not in faba bean. *Plant, Cell & Environment*, 46, 2046–2060. https://doi.org/10.1111/pce.14587